A highly efficient carboxyl-terminated hybrid adsorbent composite matrix for the adsorption of uranium(VI) and thorium(IV) from aqueous solutions and nuclear industry effluents

Thayyath Sreenivasan Anirudhan*, Sreenivasan Rijith, Vijayakumari Raveendran Nair Ratheesh

Department of Chemistry, University of Kerala, Kariavattom, Trivandrum 695 581
Email: tsani@rediffmail.com

ABSTRACT

A novel hybrid adsorbent composite matrix, polymethacrylic acid-grafted chitosan/bentonite (PMAA-g-CTS/B) was prepared through graft copolymerization reaction of methacrylic acid and chitosan in the presence of bentonite and *N,N'*- methylenebisacrylamide as cross linker. The composite was characterized using FTIR, XRD, XPS, surface area analyzer and Zeta potential measurements. Batch experiments were conducted to evaluate the efficiency of PMAA-g-CTS/B for the removal of U(VI) and Th(IV) from aqueous solutions. The adsorption behavior of the composite towards U(VI) and Th(IV) from simulated nuclear industry wastewater and seawater was studied using batch process. The adsorption behavior of PMAA-g-CTS/B towards U(VI) and Th(IV) from water and sea water was studied under varying operating conditions of pH, concentration of U(VI) and Th(IV), contact time, and temperature. The effective range of pH for the removal of U(VI) and Th(IV) was 5.0–6.0. Kinetic data followed a pseudo-second-order model. The equilibrium data were correlated with the Langmuir isotherm model. The equilibrium sorption capacity was estimated to be 117.2 for U(VI) and 110.5 mg/g for Th(IV) at 30°C. Adsorption-desorption experiments over four cycles illustrate the feasibility of the repeated uses of this composite for the extraction of U(VI) and Th(IV) from aqueous solutions. The finding of the investigation showed that the composite exhibits high adsorption capacity for U(VI) as well as Th(IV) ions.

Keywords: Chitosan; Bentonite; Composite; Graft copolymerization; Adsorption; Desorption; Uranium(VI) and Thorium(IV)

1. Introduction

Uranium and Thorium are the most valuable metals in sea water and wastewater. A number of techniques including chemical precipitation, coprecipitation, solvent extraction, ion exchange, membrane dialysis, chromatographic extraction, and adsorption have been developed to recover U(VI) and Th(IV) from aqueous solutions [1–7].

At low concentrations, the recovery of these metals is more effectively implemented by ion exchange or adsorption on solid adsorbent [8]. The composite ion exchangers have been used in several studies for the treatment of low and medium level liquid radioactive wastes [9]. The adsorbent composites with eco-friendly property and biodegradability are developed in the world. Particularly, the natural materials, such as starch, cellulose and chitosan have attracted great attention due to their abundant resources and degradability [10,11].

*Corresponding author.

The uranium and thorium concentrations in seawater were found to vary ranging from 1.80 to 4.1 and 0.14 to 0.88 µg/l, respectively [12]. The concentration of uranium in sediment samples was reported to range from 3.00 to 6.60 µg/g while those of thorium were slightly lower ranging from 0.01 to 0.68 µg/g. The economic viability of recovery of uranium and thorium from seawater still critically depends upon the kinetics of sorption in functionalized sorbents. It is desirable that the uranium and thorium species present in seawater should be instantaneously sorbed when it comes in contact with the surface of a sorbent. Therefore, the major challenge for making these radionuclide recoveries economically viable is to develop a sorbent that has a very high sorption rate. In order to enhance the kinetics of metal sorption, carboxyl groups have been anchored in the variety of substrates with different co-monomers.

Chitosan (CTS) is a biopolymer obtained by deacetylation of naturally occurring biopolymer chitin, which is abundant in nature, principally in shells of crustaceans, terrestrial invertebrates and fungi [13,14]. Recently, there has been growing interest in the chemical modification of CTS in water to improve its solubility and widen its applications. Graft copolymerization of vinyl monomers onto CTS using free radical initiator has attracted the interest of many scientists in the last decade. Bentonites are able to provide adequate particle dispersion which is necessary to obtain an uniform and stable system. The composite formation will lead to the increase in the surface area and porosity of the material. The use of materials with surface functional groups, such as amidoxime and carboxyl groups, shows improved selectivity for the adsorption of heavy metals in aqueous systems. The objective of this work is to determine the feasibility of using poly (methacrylicacid-grafted CTS/bentonite (PMAA-g-CTS/B) composite matrix as an adsorbent for the recovery of U(VI) and Th(IV) ions from water and nuclear industry wastewater. It was proposed to take advantage of the cation exchange capacity of the carboxyl group from the adsorbent surface to recover U(VI) and Th(IV) ions from aqueous solutions.

2. Experimental procedure

2.1. Materials and methods

Analytical grade chemicals were used throughout the investigation. Aqueous standard stock solution of U(VI) and Th(IV) were prepared by dissolving an accurate weighted amount of $UO_2(NO_3)_3 \cdot 6H_2O$ and $Th(NO_3)_4 \cdot 5H_2O$ (Fluka), respectively, in distilled water so as to yield a metal ion concentration of 1000 mg/l. All the required standard working solutions were prepared by diluting the stock solution with distilled water.

The methacrylic acid (MAA) and CTS were obtained from Fluka, Switzerland. Analytical grade potassium persulfate (KPS), N,N′-methylenebisacrylamide (MBA) and the chromogenic reagent Arsenazo-III were procured from E-Merck, India. Ltd. Clay used for this work is natural bentonite clay (B) obtained from M/S Ashapura Clay Mines, Gujarat, India. The commercial ion exchanger, Amberlite IRC-50 with carboxylate functionalities was obtained from Fluka, Switzerland.

2.2. Preparation of adsorbent

Scheme 1 represents the general procedure adopted for the preparation of adsorbent. The persulphate initiator decomposed on heating to generate sulfate anion radical $S\dot{O}_4^{2-}$. This anionic radical abstracts hydrogen radical from hydroxyl group of the CTS to form active sites on the CTS backbone. These active sites interact with monomer to form graft copolymer. Since a crosslinking agent (MBA) is in the system, a composite polymer matrix is formed with free COOH groups at the chain end. The inorganic bentonite particles in the composite acted as filler which enhances the mechanical strength. CTS was the starting material for the preparation of PMAA-g-CTS/B composite. 5.0 g of CTS in 30 ml distilled water is taken in a three neck round bottom flask, and MAA (15 ml) was added to it. The content was stirred well using magnetic stirrer for 15 min. 2.5 g Bentonite soaked into 15 ml water was added to it and then add 0.75 g MBA. To initiate the reaction add 0.5 g KPS and kept the mixture for 6 h at 60°C in N_2 atmosphere. The polymer obtained was then washed with distilled water until it is free from homopolymer. The product was dried at 60°C and then sieved to obtain 80–230 mesh sizes.

2.3. Equipments and method of characterization

The IR spectra of the adsorbent materials were taken by using a Perkin Elmer 1800 model IR spectrophotometer. pH measurements were made on a µ processor Systronic pH meter (model 361), XRD patterns of the adsorbent samples were obtained with a Siemens D 5005 X-ray unit using Ni-filtered Cu K_α radiation. The electrophoretic mobility measurements, µE, were carried out using a Zeta Meter system 3.0 Plus (Zeta Meter Inc., USA). Residual concentrations of U(VI) and Th(IV) after adsorption were analyzed spectrophotometrically by monitoring the absorbance using UV-Visible spectrophotometer (Jasco model V 530). The specific surface area of the CTS and PMAA-g-CTS/B was measured by BET N_2 adsorption using a Quantasorb surface area analyzer ($Q_{S/7}$) at 77 K and the data were interpreted using BET equation. A Labline temperature controlled water bath shaker with
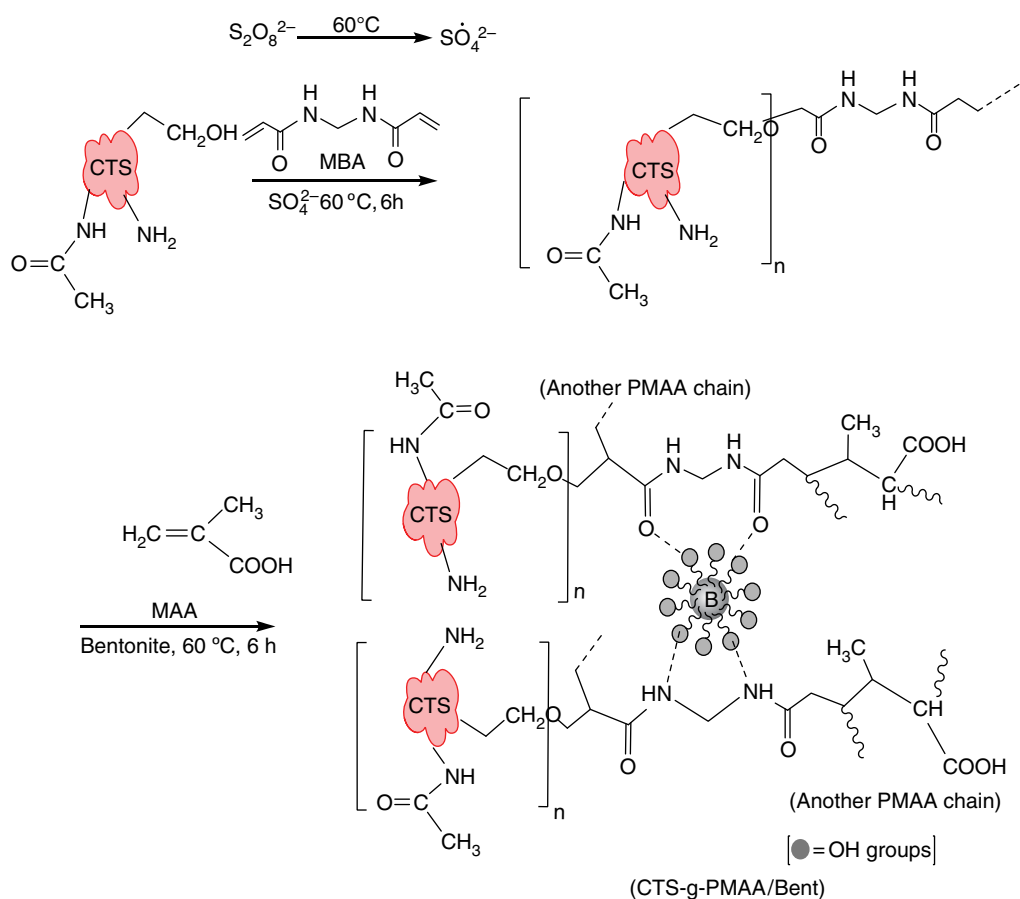
Scheme 1. Proposed mechanistic pathway for synthesis of PMAA-g-CTS/B.

a temperature tolerance of ±1.0°C was used in the equilibrium studies. The X-ray photoelectron spectroscopy (XPS) analyses were carried out with an ESCALAB Mk II under the conditions of high vacuum (10^{-7} Pa) MgK_{α} radiation with an energy of 1253.6 eV was a utilized. XPS peaks were decomposed into subcomponents using a Gaussian (80%) - Lorentzian (20%) curve fitting program, XPS peak fit, version 4.1 with a non linear background.

2.4. Adsorption experiments

Batch adsorption experiments were performed by shaking a known amount of PMAA-g-CTS/B to a series of Erlen meyer flasks containing 50 ml solutions of desired U(VI) and Th(IV) concentrations to study the extent of U(VI) ad Th(IV) adsorption. In order to optimize the removal conditions, the effects of pH, contact time, initial concentration, adsorbent dosage and reusability of the adsorbent were comprehensively tested. The pH of solutions was adjusted by using 0.1 M HCl or 0.1 M NaOH solutions before adsorption analysis. For the adsorption isotherm experiments, the initial solution

pH was 5.5 for U(VI) and Th(IV), while the initial concentration in the solution varied between 100 and 500 mg/l. The flasks were shaken in a thermostatic shaker for 3 h with the mixing rate of 200 rpm and the solid phase was separated by centrifugation. The exact concentration of U(VI) and Th(IV) ion remaining in the supernatant was determined by using UV visible spectrophotometric method. The amount of metal ion sorbed at time t (q_t), was calculated from the mass balance equation

$$q_e = \frac{(C_0 - C_e)V}{m}$$

where C_0 and C_e are the initial and equilibrium concentrations (mg/l) respectively, m is the mass of PMAA-g-CTS/B (g) and V is the volume of the solution (l). The chance of sorption of both U(VI) and Th(IV) on the walls of the containers was taken into account by conducting adsorption experiments with and without adsorbent, C_0 was measured by employing a blank test. From the results there is no significant sorption of both metals on the walls of the container.

2.5. Desorption and regeneration

The Desorption and regeneration of adsorbent is a most important aspect of an economical technology. After performing adsorption experiments with 100 mg/l U(VI) and Th(IV) solutions, the resulting metal-loaded PMAA-g-CTS/B composites were filtered and washed. The spent adsorbents were gently washed to remove the unadsorbed U(VI) and Th(IV) ions. The exhausted adsorbent was reintroduced to the desorption medium and agitated for 2 h. Qualitative estimation of metals in the desorption medium was done. A comparison of the value with those observed in the initial sorption step was used to compute the percentage recovery values, thereby checkout the long term adsorption performance of PMAA-g-CTS/B.

3. Results and discussion

3.1. Adsorbent characterization

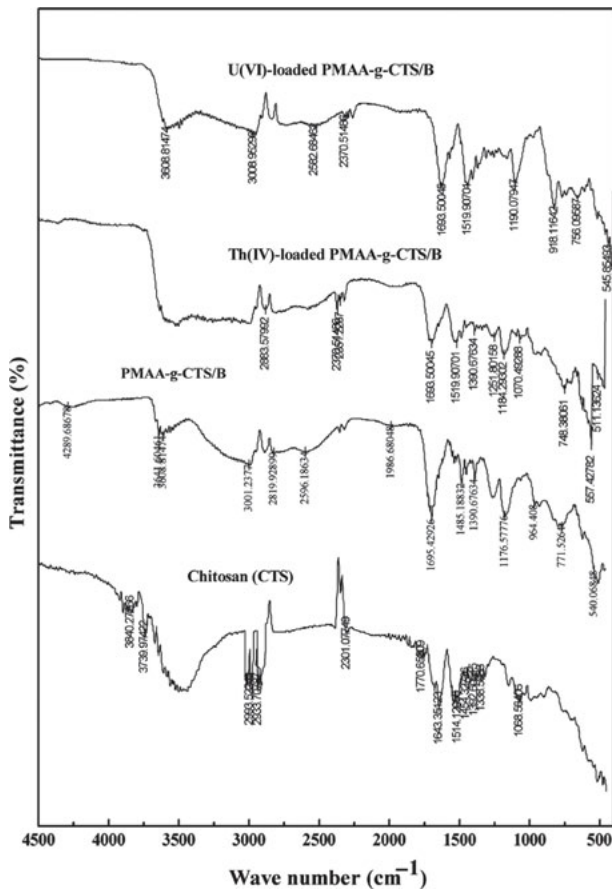The IR spectra of CTS, PMAA-g-CTS/B, U(VI) loaded-PMAA-g-CTS/B and Th(IV) loaded-PMAA-g-CTS/B are shown in Fig. 1. The broad band in the region between 3000 and 3700 cm^{-1} is due to overlapping of the stretching frequencies of –OH and–NH$_2$ groups and the peak at 1091.7 cm^{-1} corresponds to the symmetric stretching of –C-O-C- groups in CTS backbone. After CTS was grafted with MAA, the spectrum exhibits many alternations. The bands at 1695 cm^{-1} (νC–O) and 1450 cm^{-1} (νC–O) corresponds to the presence of –COOH group in the polymer composite. The peak at 1392.6 cm^{-1} corresponds to –C-N group. An obvious change in the peak position and intensity at 900–500 cm^{-1} region of the U(VI)-loaded PMAA-g-CTS/B and Th(IV)-loaded PMAA-g-CTS/B spectrum could be assigned to the formation of U–O, O-U-O, Th–O and O-Th-O bond. In metal loaded PMAA-g-CTS/B distinct peaks at 918.1 cm^{-1} and changes in peak position and intensity around 550–1000 cm^{-1} can be assigned to asymmetric stretching vibration of metal-oxygen and stretching vibration of weakly bonded oxygen atom with U(VI) and Th(IV) [15].

The diffractograms of CTS, PMAA-g-CTS/B, U(VI)-loaded PMAA-g-CTS/B and Th(IV)-loaded- PMAA-g-CTS/B (Fig. 2) are compared to determine the change in crystallinity as a result of polymerization and sorption process. The XRD pattern of CTS shows two strong peaks at 2θ = 9.34° and 19.80° with their crystal lattice constant corresponding to 8.470 and 4.075. The peak at 19.8° is attributed to the allomorphic tendon form of CTS. However, the peaks around 9.34° of CTS disappeared and the diffraction peak corresponding to

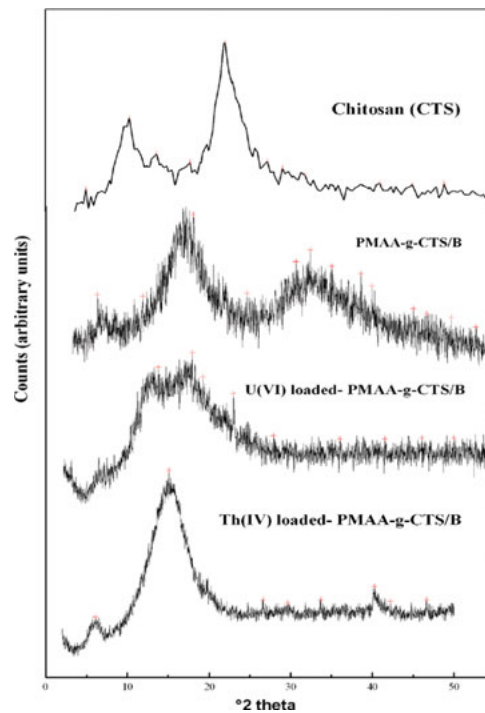Fig. 1. FTIR spectra of CTS, PMAA-g-CTS/B, U(VI) loaded-PMAA-g-CTS/B and Th(IV) loaded- PMAA-g-CTS/B.

Fig. 2. XRD patterns of CTS, PMAA-g-CTS/B, U(VI)-loaded PMAA-g-CTS/B and Th(IV)-loaded- PMAA-g-CTS/B.

$2\theta = 19.80°$ of CTS becomes gradually lowered in the XRD pattern of PMAA-g-CTS/B and the diffraction angle deviated farther and farther accordingly. It is obvious that the presence of interaction between MAA and CTS prevents or disturbs CTS from crystallization by comparison with the diffraction pattern of CTS with that of polymer blend. The intensity of peaks on the diffraction pattern of PMAA-g-CTS/B also indicates that the crystallinity decreases after functionalization. The change in width at $2\theta = 16.48°$ shows that there is a substantial decrease in crystallinity and d spacing of PMAA-g-CTS/B due to polymerization.

After U(VI) loading, new peaks observed at 6.08°, 12.16°, 16.32° and 20.9° are due to the metal complexation which tends to increase the basal spacing in PMAA-g-CTS/B. Smaller reflection at $2\theta = 6.08°$ due to the increased basal spacing of CTS monolayers over the PMAA-g-CTS/B surface during metal complexation. The broad peaks in PMAA-g-CTS/B observed at $2\theta = 29.54°$ and 36.36° were disappeared due to the rearrangement of polymer backbone over the exfoliated clay surface due to metal loading process.

To fully understand the adsorption mechanism of U(VI) onto PMAA-g-CTS/B, XPS spectra were obtained for PMAA-g-CTS/B before and after U(VI) adsorption. It has been well demonstrated that when an adsorbate was adsorbed on the adsorbent through chemical interactions, the chemical state of the atoms involved on the surface of the adsorbent could be changed, resulting a subtle change in the xps spectra for the same atom before and after adsorption takes place [16]. Fig. 3 shows the wide scan and curve fitted high resolution XPS spectrum of PMAA-g-CTS/B, U(VI)-loaded PMAA-g-CTS/B and Th(IV)-loaded PMAA-g-CTS/B. The C 1s spectrum of PMAA-g-CTS/B can be assigned to peaks at the binding energies of 286.01, 286.8, 287.1 and 290.6 eV for the carbon atoms in the C–N, C–O, methylene carbon attached to oxygen($–O–CH_2–$) and carboxyl group, respectively [17,18]. The peak appeared at 286.01 is not changed after U(VI) coordination with PMAA-g-CTS/B elucidate that the carbon from the amino group not involved in U(VI) coordination with PMAA-g-CTS/B. The PMAA-g-CTS/B shows a peak at 286.8 eV which slightly shifted to a binding energy value of 286.9 eV, this indicates the declining of electron density of carbon in carboxyl group during metal complexation reaction. Apart from the other two peaks, U(VI)-loaded- PMAA-g-CTS/B shows a shoulder peak at 291.1 eV with high intensity and peak area. This also designate the decrease in electron density around the carbon in carbonyl group of carboxylic acid moieties due to U(VI) coordination [19,20].

The wide scan O 1s spectrum of PMAA-g-CTS/B shows peaks at the binding energies of 533.57, 534.57, 534.72 and 536.08 eV, corresponding peaks for U(VI)-loaded- PMAA-g-CTS/B were at 533.80, 534.66, 534.58 and 536.1 eV. All the peaks represent the carbonyl group from carboxylic acid and amide functionalities. According to the binding energies of first three peaks of U(VI)-loaded-PMAA-g-CTS/B illustrates the decrease in electron density of oxygen in carbonyl group of carboxylic acid and amide functionalities. The peak at 536.1 eV was attributed to the oxygen from uranyl groups. These results clearly indicate the metal electron transfer existing between the oxygen from carboxylic acid in PMAA-g-CTS/B and U(VI).

Fig. 3 also contains U $4f_{5/2}$ and U $4f_{7/2}$ satellite peaks that are respectively centered at 394.03 and 383.17 eV with a splitting of about 10.8 eV. It designate the contribution of U(VI) over the surface of PMAA-g-CTS/B [17]. The region around 336.0 eV to 346.0 eV is associated with a Th(IV) satellites for Th $4f_{5/2}$ and Th $4f_{7/2}$ and is positively correlated to the Th(IV) primary peaks. However the binding energy of O 1s increases slightly from 534.05 eV to 535.02 eV in Th(IV)-loaded-PMAA-g-CTS/B, which indicates the electron transfer exists between the Th(IV) species and oxygen atom from carboxyl group.

The values of zeta potential (ζ) for CTS and PMAA-g-CTS/B were determined and were found to be 9.0 and 5.3, respectively. The decrease in ζ after modification indicates that the surface becomes more negative and this helps to adsorb positively charged U(VI) and Th(IV) ions through electrostatic interaction. The surface area was found to be 13.4 m^2/g for CTS and 29.7 m^2/g for PMAA-g-CTS/B. The values of cation exchange capacity of CTS and PMAA-g-CTS/B were found to be 1.54 and 2.24 meq g^{-1} respectively. The density of CTS and PMAA-g-CTS/B was found to be 0.8 and 1.33 g/ml, respectively. The CTS is undergo surface modification, the surface area of PMAA-g-CTS/B becomes considerably high due to most of the pores and surface moieties and functionalized with acrylic groups and the clay particles are uniformly covered with functional groups.

3.2. Effect of pH on adsorption capacity

The initial pH value of the solution is an important factor that must be considered during sorption studies. Therefore, experiments were performed in order to investigate the effect of pH on U(VI) and Th(IV) removal by varying the pH from 2.0 to 9.0 using initial concentrations of 100, 150 and 250 mg/l and an adsorbent dose of 2 g/l (Fig. 4). The maximum adsorption of U(VI) and Th(IV) was observed at pH range 4.0–6.0. A maximum adsorption of 99.2% for U(VI) and 99.6% for Th(IV) occurs at an initial concentration of 100 mg/l. At this pH range various oligomeric and monomeric hydrolyzed species of U(VI) such as $UO_2(OH)^+$ and $(UO_2)_2(OH)_2^{2+}$,
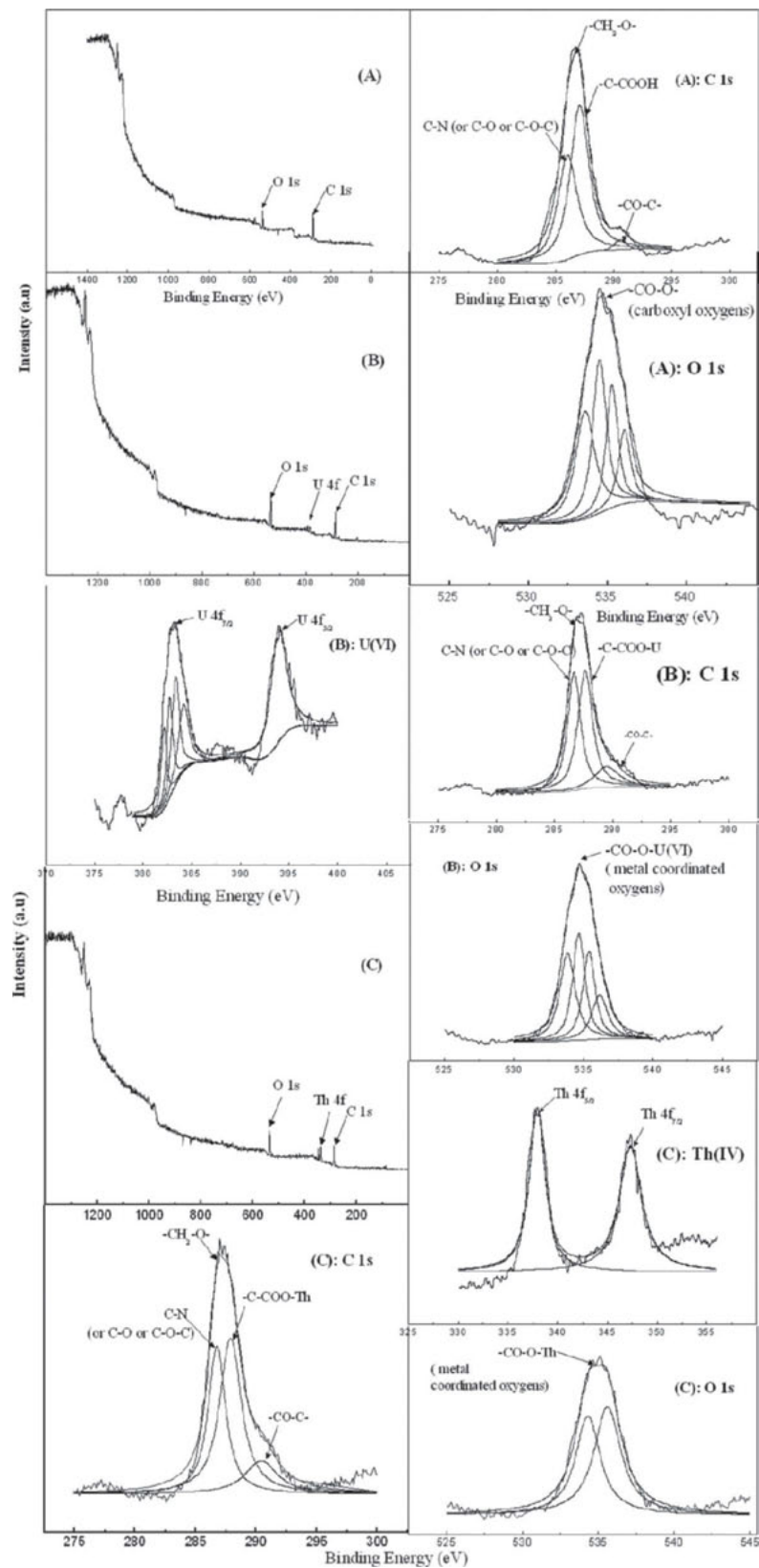
Fig. 3. XPS full scans for PMAA-g-CTS/B (A), U(VI)-loaded-PMAA-g-CTS/B (B) and Th(IV)-loaded-PMAA-g-CTS/B (C). Curve fitted high resolution scans of C1s and O1s for PMAA-g-CTS/B (A) and C1s, O1s, U(VI) and for U(VI)-loaded PMAA-g-CTS/B (B) and C1s, O1s, Th(IV) and for Th(IV)-loaded PMAA-g-CTS/B (C).
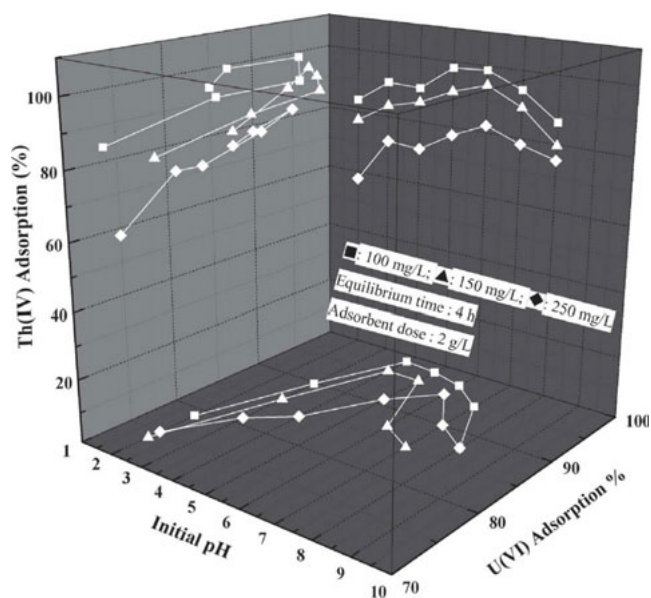
Fig. 4. Effect of pH on the adsorption of U(VI) and Th(IV) ions onto PMAA-g-CTS/B.

and for Th(IV) hydrolysis species such as $[Th(OH)_2]^{2+}$, $[Th(OH)]^{3+}$, $[Th(OH)_3]^+$ species coexist with one another [21]. The species complexed with carboxylate terminus on the adsorbent back bone after the replace of H$^+$ ions from the adsorbent surface. The adsorption behavior of the carboxyl functionalized adsorbent towards metal ion removal depends on the protonation and deprotonation properties of acidic moieties, accordingly the adsorption behavior is greatly affected by pH values. The results present in Fig. 4 elucidate that at initial pH values (pH<4.0) the adsorption capacity was lower due to the competition between hydroxonium ions (H$_3$O$^+$) with the uranyl and thorium cations for the adsorption sites of PMAA-g-CTS/B.

The point of zero charge (pHpzc) of PMAA-g-CTS is 4.3 which indicates that above pH 4.3, the PMAA-g-CTS/B surface charge is negative and below 4.3, the surface is positive. Hence above pH 4.3, the U(VI) and Th(IV) ion adsorption on PMAA-g-CTS/B surface occurs through electrostatic interactions. When the pH is higher than 6.0, in the solution will be precipitated and will change the existing state of in the solution to form neutral, and anionic form, of U(VI) species [22]. Therefore it seems that the pH of solution used for further adsorption studies should be lower than 6.0 and initial pH of 5.5 was selected as optimum for all further studies optimized. In the case of Th(IV) the maximum adsorption shown in the pH range 4.0–6.0, may be due to the formation of Thorium(IV) complexes with carboxyl groups, because of its stability constant with Th(IV) is high [23].

3.3. Effect of contact time and initial concentration

Batch kinetic experiments were performed to determine the time required for U(VI) and Th(IV) adsorption process to reach equilibrium and the kinetic results were presented in Fig. 5. The effect of contact time on adsorption of U(VI) and Th(IV) onto PMAA-g-CTS/B was studied over a time of 0–240 min using different initial concentrations (100–250 mg/l). Fig. 5 shows that the amount of U(VI) and Th(IV) adsorbed per unit mass of adsorbent increased rapidly within 30 min and slowly reaches the saturation at about 3 h respectively for U(VI) and Th(IV). After this equilibrium period, the amount of metal adsorbed did not change significantly with time due to quick exhaustion of adsorbent. The amount
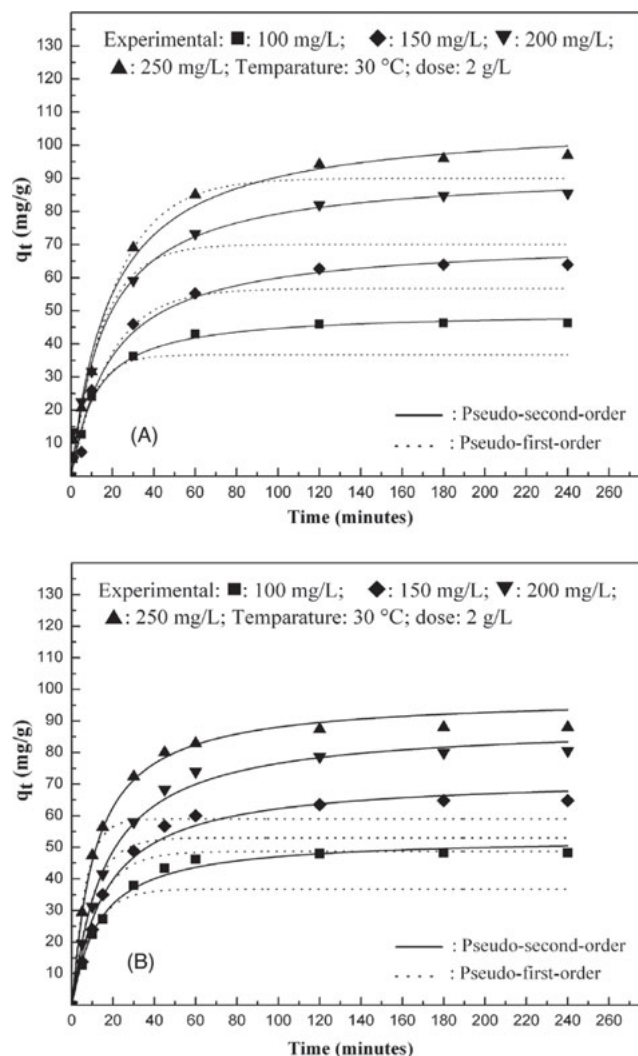

Fig. 5. Effect of initial concentration and contact time on the adsorption of U(VI) onto PMAA-g-CTS/B (A) and Th(IV) onto PMAA-g-CTS/B (B) and comparison of observed data with pseudo-second-order and pseudo-first-order kinetic model.

of metal adsorbed versus times curves are smooth and continuous. The time profile of Th(IV) uptake is a single, smooth and continuous curve leading to saturation, suggesting the cooperativity of U(VI) and Th(IV) on the surface of the adsorbent. The equilibrium time of 3 h can be considered very short, which is an economically favorable condition for the adsorbent described here. The removal efficiency increased from 49.01 to 102.24 mg/g for U(VI) and 51.15 to 97.81 mg/g for Th(IV) as initial concentration increased from 100 to 250 mg/l, respectively.

The results show that an increase in the initial concentration leads to an increase in the U(VI) and Th(IV) uptake. The data indicate that the initial metal ion concentration determines the equilibrium concentration and also determines the uptake rate of U(VI) and Th(IV) and the kinetic character of metal uptake [24]. The rate parameters are depicted in Table 1. This might be due to the fact that increasing U(VI) and Th(IV) concentration increased the number of collision between the adsorbent and metal ion species, this leading an increased metal uploading [25]. Results clearly indicate that the rate of adsorption of U(VI) and Th(IV) onto PMAA-g-CTS/B depend on the initial concentration.

3.3.1. Adsorption kinetics

To interpret the experimental kinetic data properly, it is necessary to determine the steps in the adsorption process, governing the overall removal rate for the system. Also, the rate-limiting step is important in the field application point of view. The rate-limiting step of the adsorption process can be calculated using the pseudo-first-order and pseudo-second-order kinetic equations [26].

The non linear kinetic equations may be written as:

Pseudo-first-order: $q_t = q_e(1 - e^{-k_1 t})$;

Pseudo-second-order: $q_e = \dfrac{k_2 q_e^2 t}{1 + k_2 q_e t}$

where q_e and q_t (mg/g) are the adsorption capacities at equilibrium and at time t respectively. k_1 (min^{-1}) and k_2 (g/mg/min) are pseudo-first-order and pseudo-second-order rate constants, respectively. The values of k_1 and k_2 were obtained from non linear regression analysis. The values of k_1 were found to be increased from 9.1×10^{-2} to 16.2×10^{-2} min^{-1} for U(VI) and 0.1×10^{-2} to 9.8×10^{-2} min^{-1} for Th(IV) while pseudo-second-order rate constants were found to be decreased from 1.43×10^{-3} to 0.54×10^{-3} g/mg/min for U(VI) and 1.75×10^{-3} to 0.49×10^{-3} g/mg/min for Th(IV) when initial U(VI) and Th(IV) concentration increased from 100 to 250 mg/l (Table 1). From Table 1 it can be seen that the values of χ^2 for pseudo-first-order kinetic model are very high and R^2 values are very less. However, there are large differences between the the experimental q_e values(q_e, exp) and the calculated q_e values (q_e, cal), which indicate that the pseudo-first-order kinetic model was poor fit for the adsorption process of PMAA-g-CTS/B polymer composite for U(VI) and Th(IV). It can also be found from Table 1 that χ^2 and R^2 for the pseudo-second-order kinetic model are more favourable, moreover the q_e, cal values for the pseudo-second-order kinetic model are all consistent with q_e, exp values. These results suggest that the adsorption processes of PMAA-g-CTS/B composite matrix for the recovery of U(VI) and Th(IV) from aqueous media can be well described by the pseudo-second-order kinetic model.

3.4. Adsorption isotherm study

The results of the U(VI) and Th(IV) adsorption isotherm experiments are shown in Fig. 6. The adsorption capacity considerably increased with equilibrium concentration and temperature. In order to optimize the design of an adsorption system to remove U(VI) and Th(IV) from aqueous solutions using PMAA-g-CTS/B,

Table 1
Kinetic parameters for the adsorption of U(VI) onto PMAA-g-CTS/B and Th(IV) onto PMAA-g-CTS/B at different concentrations

|	Pseudo-first-order					Pseudo-second-order			
	q_e exp (mg/g)	$k_1 \times 10^{-2}$ (min^{-1})	$q_e$cal (mg/g)	R^2	χ^2	$k_2 \times \omega 10^{-3}$ (g/mg/min)	q_e cal (mg/g)	R^2	χ^2
Conc. of U(VI) (mg/l)									
100	49.01	0.1	36.68	0.88	40.0	1.75	47.18	0.99	1.77
150	68.21	5.3	56.72	0.96	24.8	0.73	64.96	0.98	10.30
200	86.03	6.7	70.03	0.92	80.6	0.65	84.08	0.99	11.50
250	102.24	4.8	90.02	0.98	20.43	0.49	99.87	0.99	14.20
Conc. of Th(IV) (mg/l)									
100	51.15	9.8	36.78	0.81	60.62	1.43	53.18	0.99	3.1
150	73.91	8.4	48.68	0.89	110.61	0.85	72.32	0.98	7.5
200	82.31	10.4	53.28	0.85	168.2	0.69	84.08	0.99	5.6
250	97.81	16.2	59.21	0.88	211.1	0.54	94.51	0.99	6.3
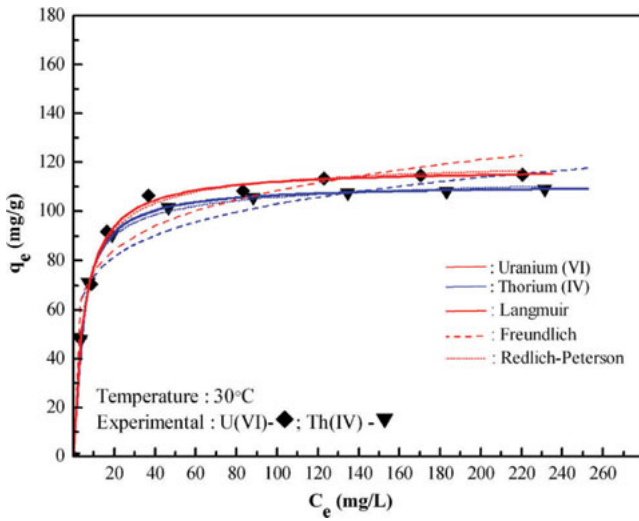
Fig. 6. Comparison of the experimental and model fits of Langmuir, Freundlich and Redlich-Peterson isotherm for the adsorption of U(VI) and Th(IV) onto PMAA-g-CTS/B at 30°C.

it is important to establish the most appropriate correlation for the equilibrium curves. The Langmuir, Freundlich and Redlich-Peterson models are often used to describe equilibrium adsorption isotherms. Equilibrium data, commonly known as adsorption isotherms, are the basic requirements for the design of adsorption systems.

Obtaining equilibrium data for a specific adsorbate/adsorbent system can be performed experimentally, with a time-consuming procedure that is incompatible with the growing need for sorption systems design. Analysis of equilibrium data is important for developing an equation that can be used to compare different sorbents under different operational conditions and to design and optimize an operating procedure [27].

Langmuir: $q_e = \dfrac{Q_0 b C_e}{1 + b C_e}$;

Freundlich: $q_e = K_F C_e^{1/n}$;

Redlich–Peterson model: $q_e = \dfrac{K_R C_e}{1 + b C_e^{\beta}}$

where C_e is the equilibrium concentration of the uranium on adsorption in mg/l and q_e is the amount adsorbed at equilibrium in mg/g. Q_0 and b are the Langmuir constants related to adsorption capacity and energy of adsorption, respectively. K_F and $1/n$ are Freundlich constants related to adsorption capacity and intensity of the adsorption respectively. K_R, β and b are Redlich-peterson isotherm constants related to adsorption capacity, empirical exponent and energy of adsorption, respectively. The values of isotherm constants were determined using nonlinear regression analysis. The adsorption capacity Q_0 increases with increase in temperature. It has increased from 99.9 to 126.6 mg/g and 111.9 to 130.3 mg/g respectively for

Th(IV) and U(VI) adsorption with rise in temperature from 20 to 50°C. The values of b increased from 0.24 to 0.46 1/mg for U(VI) and 0.09 to 0.35 1/mg for Th(IV) with rise in temperature from 20 to 50°C. This indicates that adsorption rate increases with increase in temperature. It should be noted that β normally lying between 0 and 1, indicated a favorable adsorption for the studied adsorbent. Among these adsorption models, the best correlations were observed for Langmuir model.

From the values of R^2 and χ^2 demonstrated the agreement of the experimental data with the Langmuir model very well for the adsorption of U(VI) and Th(IV) onto PMAA-g-CTS/B. The fact that the Langmuir isotherm fits the experimental data very well may be due to homogeneous distribution of active sites on PMAA-g-CTS/B, since the Langmuir equation assumes that the surface is homogeneous.

3.5. Effect of adsorbent dose with simulated nuclear industry wastewater and sea water

Batch equilibrium experiments were performed to test the effectiveness of PMAA-g-CTS/B composite to recover U(VI) from simulated nuclear industry wastewater sample and Th(IV) from simulated seawater sample (Fig. 7). The amount of adsorbent concentration was varied from 1.0 to 10.0 g/l at a constant pH of 5.5 using simulated nuclear industry wastewater, having the composition: U(VI) (100 mg/l), 1.248 g Na_2SO_4, 0.278 g $CaCl_2$, 1.055 g $Mg(NO_3)_2$, 0.12 ml H_3PO_4, 0.967 g $(NH_4)_2C_2O_4$ [28]. For the quantitative removal of from 100 mg/l U(VI) from simulated nuclear industry wastewater, a optimum adsorbent dose of 2 g PMAA-g-CTS/B was required, while the dose requirement of bentonite, CTS,
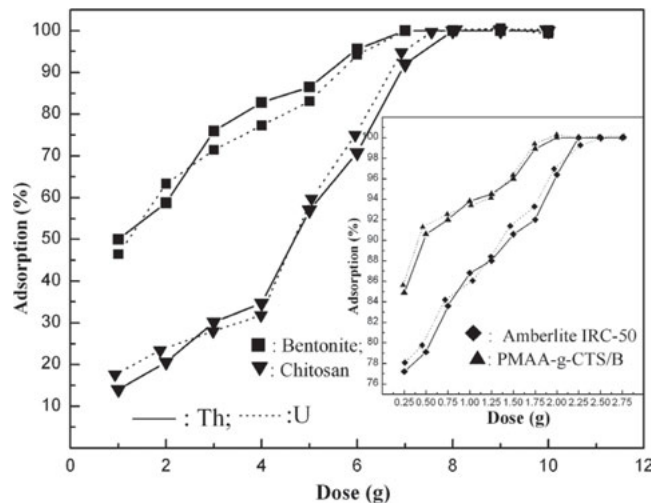

Fig. 7. Effect of adsorbent dose on the adsorption of U(VI) and Th(IV) ions onto PMAA-g-CTS/B.

and Amberlite IRC-50 was 7.0, 8.0 and 2.5 g respectively. The results clearly show that PMAA-g-CTS/B is more effective than bentonite, CTS, and Amberlite IRC-50.

Batch equilibrium experiments were performed to test the effectiveness of PMAA-g-CTS/B composite to recover Th(IV) in sea water sample. Th(IV) containing (100 mg/l) simulated sea water sample having the composition NaCl (82.52 g/l), Na_2SO_4 (13.91 g/l), KCl (2.35 g/l), $NaHCO_3$ (0.68 g/l), KBr (0.34 g/l), H_3BO_3 (0.09 g/l), NaF (0.011 g/l), $MgCl_2 \cdot 6H_2O$ (37.60 g/l), $CaCl_2 \cdot 2H_2O$ (5.26 g/l) $SrCl_2 \cdot 2H_2O$ (0.09 g/l) was used [29]. The effect of adsorbent dose on Th(IV) removal from sea water sample was studied at different adsorbent doses ranging between 2.0 and 10.0 g/l using chitosan and Bentonite while the dose level ranging from 0.25 to 2.75 g for PMAA-g-CTS/B and Amberlite IRC-50.

The percentage removal increases with increase of adsorbent dose. For the quantitative removal of 100 mg/l Th(IV) from 1.0 l sea water, a minimum adsorbent dosage of 8.2 g CTS or 7.0 g bentonite was used. The dosage of 2.25 g Amberlite IRC-50 or 2.0 g PMAA-g-CTS/B was required for the complete removal of Th(IV) from simulated sea water. The results clearly show that PMAA-g-CTS/B is about 4.1, 3.5 and 1.13 times more effective than CTS, Bentonite and Amberlite IRC-50 respectively. It indicates the enhanced performance of PMAA-g-CTS/B over other adsorbents such as Bentonite, Amberlite IRC-50 and CTS.

3.6. Desorption and regeneration studies

The spent PMAA-g-CTS/B was regenerated by shaking the U(VI)-loaded PMAA-g-CTS/B and Th(IV)-loaded PMAA-g-CTS/B using different types of desorbing agents such as 0.1 M NaOH, 0.1 M Na_2SO_4, 0.1 M NaCl, 0.1 M $NaNO_3$, 0.1 M HCl and 0.1 M HNO_3 at room temperature. The percentage desorption for corresponding desorbing agents were 55.4, 62.2, 64.5, 68.2, 84.2, 99.4 and 56.3, 61.4, 62.9, 66.3, 82.1, 97.2%, respectively for U(VI)-loaded PMAA-g-CTS/B and Th(IV)-loaded PMAA-g-CTS/B. Among these, 0.1 M HNO_3 was proved to be the most suitable desorbing agent. The synthesized PMAA-g-CTS/B was assessed for deterioration by subjecting to repeated adsorption-desorption experiments with 0.1 M HNO_3. After four cycles, the adsorption capacity is not significantly reduced, the adsorption capacity of the PMAA-g-CTS/B decreased from 99.4% in the first cycle to 87.1% in the fourth cycle in case of U(VI)-loaded PMAA-g-CTS/B and 97.2% in the first cycle to 86.7% in the fourth cycle in case of Th(IV)-loaded PMAA-g-CTS/B. Apparently the performance of the adsorbent was not appreciably deteriorated after repeated use and regeneration for four cycles, indicating that the synthesized PMAA-g-CTS/B was mechanically and chemically robust for the

recovery of U(VI) and Th(IV) from nuclear industrial wastewater and sea water.

4. Conclusions

In the present study, a novel adsorbent, poly-(methacrylic acid)-grafted chitosan/bentonite composite (PMAA-g-CTS/B) was synthesized and characterized. Its efficiency in removing U(VI) and Th(IV) was tested by batch adsorption technique. The pH 5.5 was found to be optimum for the adsorption of U(VI) on PMAA-g-CTS/B and pH 6.0 for Th(IV) on PMAA-g-CTS/B. The best kinetic correlation for the sorption of U(VI) and Th(IV) onto PMAA-g-CTS/B under the experimental conditions investigated was provided by the pseudo-second-order kinetics. The equilibrium data could better be described by the Langmuir isotherm than Freundlich and Redlich-Peterson isotherm models. Attempts for quantitative removal of U(VI) from simulated nuclear industry wastewater and Th(IV) from simulated sea-water using variable adsorbent doses were made and satisfactory results were obtained. The spent adsorbent could be effectively regenerated by desorption with 0.1 M HNO_3 and the adsorption capacity was not found to decrease after four cycles of adsorption-desorption experiments.

References

[1] A. Mellah, S. Chegrouche and M. Barkat, The precipitation of ammonium uranyl carbonate (AUC): thermodynamic and kinetic investigations, Hydrometallurgy, 85 (2007) 163–171.

[2] F.A. Aydin and M. Soylak, A novel multi-element co precipitation technique for separation and enrichment of metal ions in environmental samples, Talanta, 73 (2007) 134–141.

[3] M.R. Yaftian, R. Taheri, A.A. Zamani and D. Matt, Thermodynamics of the solvent extraction of thoriumand europium nitrates by neutral phosphorylated, J. Radioanal. Chem., 262 (2004) 455–459.

[4] A.C.Q. Ladeira and C.A. Morais, Uranium recovery from industrial effluent by ion exchange—column experiments, Miner. Eng., 18 (2005) 1337–1340.

[5] A.T. Kuhu, Electrochemistry of Cleaner Environments, Plenum Press, New York, 1972.

[6] M.L. Dietz, H.E. Philip, L.R. Sajdak and R. Chiarizia, An improved extraction chromatographic resin for the separation of uranium from acidic nitrate media, Talanta, 54 (2001) 1173–1184.

[7] Y. Jung, S. Kim, S.J. Park and J.M. Kim, Application of polymer-modified nanoporous silica to adsorbents of uranyl ions, Colloids Surf. A., 313 (2008) 162–166.

[8] B.M. Thomson, C.L. Smith, R.D. Busch, M.D. Siegel and C. Baldwin, Removal of metals and radionuclides using apatite and other natural sorbents, J. Environ. Eng., 129 (2003) 492–499.

[9] T.S. Anirudhan and M. Ramachandran, Synthesis and Characterization of Amidoximated Polyacrylonitrile/Organobentonite Composite for Cu(II), Zn(II), and Cd(II) Adsorption from Aqueous Solutions and Industry Wastewaters, Ind. Eng. Chem. Res., 47 (2008) 6175–6184.

[10] U.R. Gosavi, R.L. Deopurkar and V.S. Ghole, Microbial Degradation of Superabsorbent HSPAN Gel by an Indigenously Isolated Bacterial Culture, Macromolecules, 32 (1999) 4264–4271.

[11] H. Hosseinzadeh, A. Pourjavadi, G.R. Mahdavinia and M.J. Zohuriaan-Mehr, Modified Carrageenan. 1, H-CarragPAM, a Novel Biopolymer-Based Superabsorbent Hydrogel, J. Bioact. Compat. Polym., 20 (2005) 475–490.

[12] S. Akyil and A.M. Yusof, The distribution of uranium and thorium in samples taken from different polluted marine environment, J. Hazard. Mater., 144 (2007) 564–569.

[13] E. Longhinotti, F. Pozza, L. Furlan, M.N.M. Sanches, M. Klug, M.C.M. Laranjeira and V.T. Fávere, Adsorption of Anionic Dyes on the Biopolymer Chitin, J. Braz. Chem. Soc., 9 (1998) 435–440.

[14] A.J. Varma, S.V. Deshpande and J.F. Kennedy, Metal complexation by chitosan and its derivatives: a review, Carbohydr. Polym., 55 (2004) 77–93.

[15] S.K. Kazy, S.K. Das and P. Sar, Lanthanum biosorption by a Pseudomonas sp.: equilibrium studies and chemical characterization, J. Ind. Microbiol., 33 (2006) 773–783.

[16] D.B. Beach, K.D. Bomben, N.M. Edelstein, D.C. Eisenberg, W.L. Jolly, R. Shinomoto and A. Streitwieser Jr, An x-ray photoelectron spectroscopic study of uranium compounds, Inorg. Chem., 25 (1986) 1735–1737.

[17] L. Dambies, C. Guimon, S. Yiacoumi and E. Guibal, Characterization of metal ion interactions with chitosan by X-ray photoelectron spectroscopy, Colloids Surf. A. Asp., 177 (2000) 203–214.

[18] A.K. Arof, N.M. Morni and M.A. Yarmo, Evidence of lithium–nitrogen interaction in chitosan-based films from X-ray photoelectron spectroscopy, Mater. Sci. Eng. B, 55 (1998) 130–133.

[19] E.S. Ilton, J.F. Boily and P.S. Bagus, Beam induced reduction of U(VI) during X-ray photoelectron spectroscopy: The utility of the U4f satellite structure for identifying uranium oxidation states in mixed valence uranium oxides, Surf. Sci., 601 (2007) 908–916.

[20] B.G. Santos, .H.W. Nesbitt., J.J. Noel.and D.W. Shoesmith, X-ray photoelectron spectroscopy study of anodically oxidized SIM-FUEL surfaces, Electrochim. Acta, 49 (2004) 1863–1873.

[21] L.I. Vodolazov, V.V. Shatalov, T.V. Molchanova and V.A. Peganov,. Polymerization of Uranyl Ions and Its Role in Ion-Exchange Extraction of Uranium, At. Energ., 90 (2001) 213–217.

[22] Z. Zhang and D.A. Clifford, Exhausting and Regenerating Resin for Uranium Removal, J. AWWA, 86 (1994) 228–241.

[23] D. Langmuir and J.S. Herman, The mobility of thorium in natural waters at low temperatures, Geochim. Cosmochim. Acta, 44 (1980) 1753–1756.

[24] A. Shukla, Y. Zhang, P. Dubey, J.L. Margrave and S.S. Sukla, The role of sawdust in the removal of unwanted materials from water, J. Hazard. Mater., 95 (2002) 137–157.

[25] Z. Aksu, Equilibrium and kinetic modelling of cadmium(II) biosorption by C. vulgaris in a batch system: effect of temperature, Sep. Purif. Technol., 21 (2002) 285–294.

[26] T.S. Anirudhan, S. Rijith and L. Divya, Preparation and application of a novel functionalized coconut coir pith as a recyclable adsorbent for phosphate removal, Sep. Sci. Technol., 44 (2009) 2774–2796.

[27] G. Bayramoglu and M.Y. Arica, Ethylenediamine grafted poly(glycidylmethacrylate-co-methylmethacrylate) adsorbent for removal of chromate anions, Sep. Purif. Technol., 45 (2005) 192–199.

[28] M. Jansson-Charrier, E. Guibel, J. Roussy, R. Surjous and P. Le Cloirec, Dynamic removal of uranium by chitosan: influence of operating parameters, Water Sci. Technol., 34 (1996) 169–177.

[29] R.P. Timothy, M. Yoshiaki and M.L. Carrol, A Manual of Chemical and Biological Methods for Sea Water Analysis, Pergamon Press. Inc, 395. New York 10523, USA, 1984.